3.1.3. ANNUAL CYCLES

The annual cycles of aerosol optical properties for the four baseline and three regional stations are illustrated in Figures 3.1 and 3.2, respectively. The data are presented in the form of box and whisker plots that summarize the distribution of values. Each box ranges from the lower to upper quartiles with a central bar at the median value, while the whiskers extend to the 5^{th} and 95^{th} percentiles. The statistics are based on hourly averages of each parameter for each month of the year; also shown are the annual statistics for the entire period of record. The horizontal line across each plot represents the annual median, so measurements above and below the median can easily be discerned. The annual cycles for the baseline stations are based on data through the end of 2001, except at SMO, where scattering measurements were made only from 1977 to 1991 and CN from 1977 to 1997. In general, changes in long-range transport patterns dominate the annual cycles of the baseline stations.

Figure 3.1 shows that, for BRW, the high values of CN, σ_{sp}, and σ_{ap} are observed during the Arctic haze period when anti-cyclonic activity transports pollution from the lower latitudes of Central Europe and Russia. A more stable polar front characterizes the summertime meteorology. High cloud coverage and precipitation scavenging of accumulation-mode (0.1- to 1.0-μm diameter) aerosols account for the annual minima in σ_{sp} and σ_{ap} from June to September. In contrast, CN values have a secondary maximum in the summer, which is thought to be the result of sulfate aerosol production from gas-to-particle conversion of dimethyl sulfide (DMS) oxidation products from local oceanic emissions [*Radke et al*., 1990]. The aerosol single-scattering albedo displays little annual variability and is indicative of highly scattering sulfate and seasalt aerosol. A September minimum is observed in Ångström exponent (*å)* when σ_{sp} and accumulation-mode aerosols are also low but when primary production of coarse-mode seasalt aerosols from open water is high [*Quinn et al.*, 2002; *Delene and Ogren*, 2002]. *Quinn et al.* [2002] have also shown, based on their chemical analysis of the submicrometer aerosol particles at BRW, that seasalt has a dominant role in controlling scattering in the winter; non-seasalt sulfate is the dominant scatterer in the spring; and both components contribute to scattering in the summer.

For MLO, the highest σ_{sp} and σ_{ap} values occur in the springtime and result from the long-range transport of pollution and mineral dust from Asia. However, little seasonality is seen in CN concentrations at MLO, indicating that the smallest particles (<0.1-μm diameter), which usually dominate CN concentration, are not enriched during these long-range transport events. At SPO, both the aerosol σ_{sp} and *å* display seasonal cycles, with a σ_{sp} maximum and an *å* minimum in austral winter associated with the transport of coarse-mode seasalt from the Antarctic coast to the interior of the continent. The summertime peaks in CN and *å* are associated with fine-mode sulfate aerosol and correlate with a seasonal sulfate peak found in the ice core, presumably from coastal biogenic sources [*Bergin et al*., 1998]. At SMO, aerosol extensive properties display no distinct seasonal variation. At BRW and MLO, albedo values above 1.0 are due to instrument noise at low aerosol concentration. These high albedo values are not present in daily averaged data. Furthermore, these high albedo values are not present if data are excluded where σ_{sp} is below 1 Mm^{-1}. Hence, the high albedo values result from an instrument detection limitation problem.

Based on only 4-7 years of measurements, the annual cycles for the regional stations (Figure 3.2) are less certain than those of the baseline stations. The proximity of the regional sites to North American pollution sources is apparent in the results, with monthly median values of σ_{sp} that are up to 2 orders of magnitude higher than values from the baseline stations. The Bondville, Illinois, site (BND), situated in a rural agricultural region, displays an autumn high in σ_{ap} and a low in ω_o that coincide with anthropogenic and dust aerosols emitted during the harvest [*Delene and Ogren*, 2002]. As evident in the lower σ_{sp} and σ_{ap} values, the Southern Great Plains site (SGP), Lamont, Oklahoma, is more remote than BND. SGP has a similar but less pronounced annual cycle with late-summer highs in σ_{sp} and σ_{ap}, and a corresponding minimum in ω_o [*Delene and Ogren*, 2002; *Sheridan et al.*, 2001]. Little seasonal variability is observed in aerosol properties at Sable Island, Nova Scotia (WSA). Values of *å* tend to be higher in the summer and very likely result from transport of fine-mode sulfate aerosol from the continent and lower coarse-mode production of particles with lower summer wind speeds [*Delene and Ogren*, 2002].

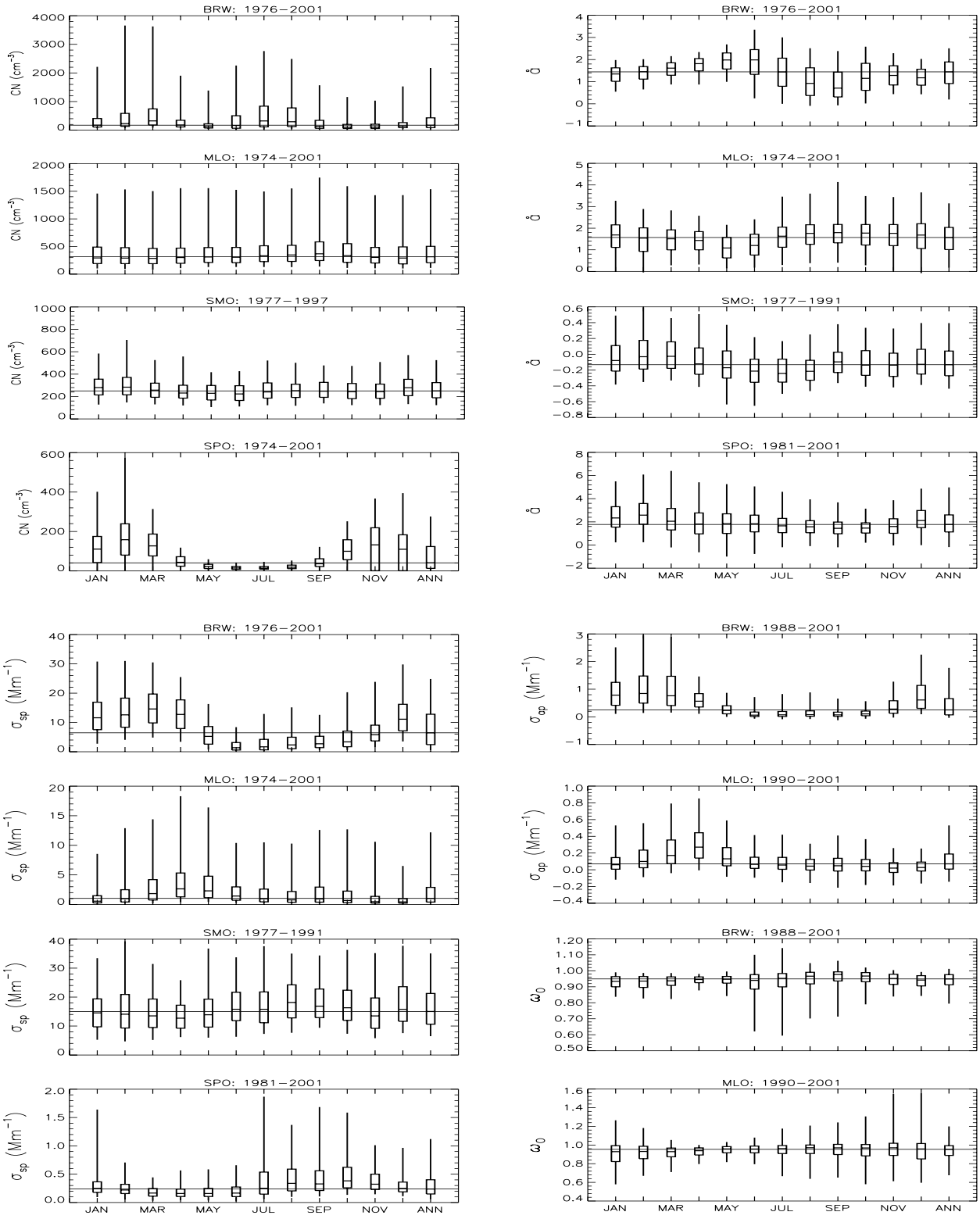

Fig. 3.1. Box and whisker plots of annual cycles showing statistics for condensation nuclei (CN) concentration, Ångström exponent (*å*), and total scattering coefficient (σ_{sp}) at baseline stations BRW, MLO, SMO, and SPO; and for absorption coefficient (σ_{ap}) and single scattering albedo (ω_0) at BRW and MLO. Statistics representing the entire period are given in the last column (ANN). Each box ranges from the 25th to 75th quartiles, and the horizontal line represents the median value. The whiskers extend to the 5th and 95th quartiles.

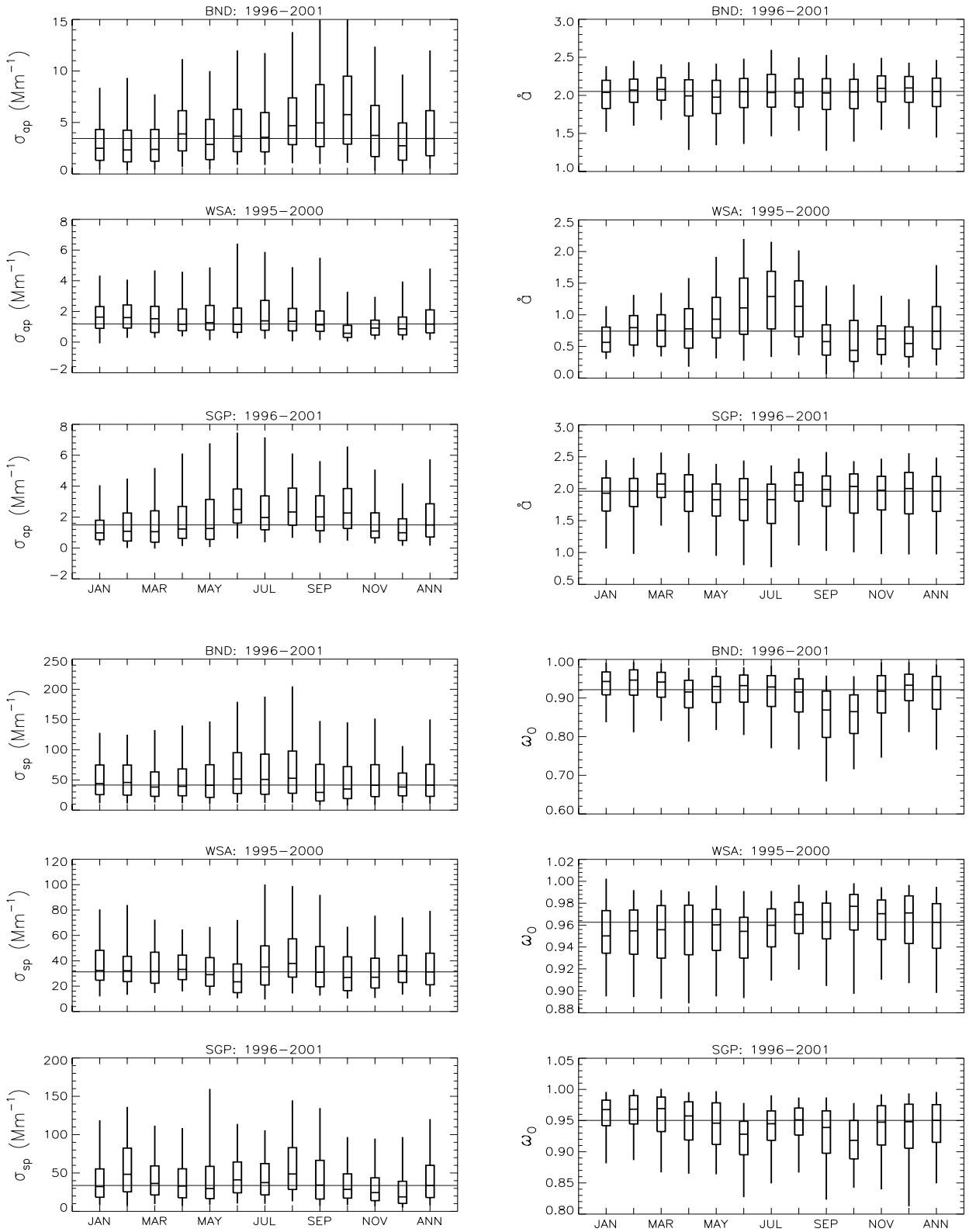

Fig. 3.2. Box and whisker plots of annual cycles for regional stations at BND, WSA, and SGP showing statistics for absorption coefficient (σ_{ap}), Ångström exponent ($\mathring{a}$), total scattering coefficient (σ_{sp}), and single-scattering albedo (ω_0). Statistics representing the entire period are given in the last column (ANN). The boxes and whiskers are as in Figure 3.1.